

# RoSMM: A Robust and Secure Multi-Modal Watermarking Framework for Diffusion Models

ZhongLi Fang

Fudan University, Shanghai, China

zlfang22@m.fudan.edu.cn

\*Yu Xie

The Purple Mountain Laboratories, Nanjing, China

\*Ping Chen

Fudan University, Shanghai, China

## Abstract

Current image watermarking technologies are predominantly categorized into text watermarking techniques and image steganography; however, few methods can simultaneously handle text and image-based watermark data, which limits their applicability in complex digital environments. This paper introduces an innovative multi-modal watermarking approach, drawing on the concept of vector discretization in encoder-based vector quantization. By constructing adjacency matrices, the proposed method enables the transformation of text watermarks into robust image-based representations, providing a novel multi-modal watermarking paradigm for image generation applications. Additionally, this study presents a newly designed image restoration module to mitigate image degradation caused by transmission losses and various noise interferences, thereby ensuring the reliability and integrity of the watermark. Experimental results validate the robustness of the method under multiple noise attacks, providing a secure, scalable, and efficient solution for digital image copyright protection.

## 1. Introduction

With the rapid rise of AIGC (Artificial Intelligence-Generated Content) [Rombach et al. \(2022\)](#)[Wallace et al. \(2023\)](#), countless synthetic images are now shared across media and the internet. While advanced models like diffusion [Nichol and Dhariwal \(2021\)](#)[Watson et al. \(2022\)](#)[Pandey et al. \(2022\)](#) meet the demand for high-quality content, their misuse has raised serious issues around data privacy, copyright protection, and social trust. New watermarking technologies [Xiong et al. \(2023\)](#)[Fernandez et al. \(2023\)](#)[Asnani et al. \(2024\)](#) provide a simple and effective way to resolve copyright disputes and track information.

Watermarking offers a direct method for tracing image

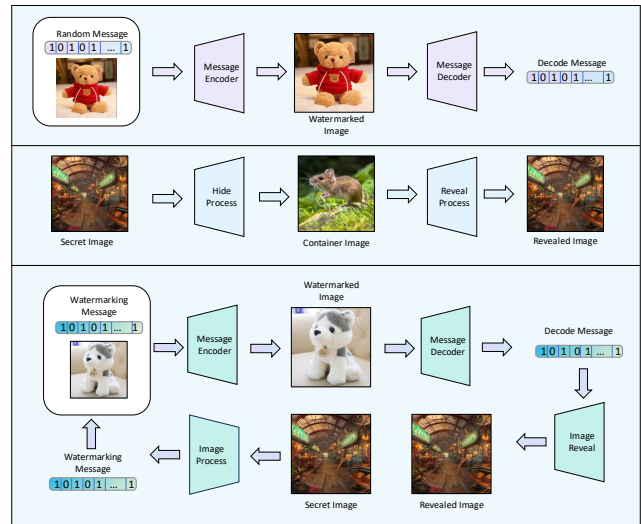


Figure 1. Current watermarking methods fall into two main categories: text-based watermarking for traceability and image steganography for embedding information. Our method goes beyond these by converting binary watermarks into more robust image-based watermarks, offering a new multi-modal approach for watermarking in image generation.

information, as it can be embedded explicitly or implicitly within generated images, providing a foundational solution for subsequent copyright protection and information traceability. Existing image watermarking techniques are generally divided into two categories: text-based watermark tracing methods [Wen et al. \(2024\)](#)[Ci et al. \(2024\)](#) and image-based steganography [Lu et al. \(2021\)](#)[Jing et al. \(2021\)](#), as illustrated in Figure 1. Image-text watermarking methods are limited in the amount of information they can convey, typically constrained to 16 to 256 bits, with recent advances [Yang et al. \(2024\)](#) achieving stable transmission of up to 512 bits, approximately 64 characters. In contrast, image steganography embeds secret images within generated im-

ages and typically requires noise-free conditions for training, making it vulnerable to real-world disturbances such as noise and non-linear transformations. These limitations hinder the practicality and applicability of image steganography in robust environments [Jaini et al. \(2019\)](#)[Papamakarios et al. \(2017\)](#).

From the above analysis, it is evident that each of these methods has distinct limitations: traditional image-text watermarking, while widely applicable, transmits only a limited amount of information, whereas image steganography can embed a complete secret image, but it involves significant computational costs and lacks robustness against external attacks. In general, existing methods struggle to balance security, robustness, and information density in watermarks. The natural question arises: is it possible to combine the security and robustness of text content watermarking with the informational density characteristic of image-based steganography?

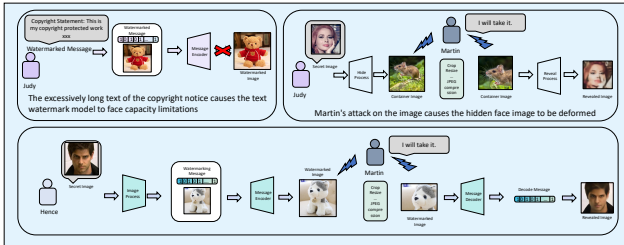


Figure 2. Applications of multi-modal watermarking. The proposed method demonstrates exceptional performance in watermark traceability, copyright protection, and secure data transmission.

The answer is affirmative. For the concept of vector discretization coding from vector quantized variational autoencoders, this paper introduces an innovative Robust and Secure Multi-Modal Watermarking framework (RoSMM) that not only enables conversion between image and text watermarks but also integrates the advantages of image steganography and text content watermarking, establishing a novel approach to multi-modal watermarking content. Additionally, to further enhance the robustness and readability of the watermark, we designed an image restoration module that performs secondary restoration processing on the watermark information, significantly enhancing the anti-interference capability of the watermark content. Overall, by combining text-based watermarking and image steganography, this framework expands the functionality and scope of watermarking techniques, providing new possibilities for watermark traceability and application versatility.

To the best of our knowledge, we are the first to address and implement the challenging task of multi-modal watermarking content, providing theoretical proof of its feasi-

bility. Moreover, this method can be integrated as a simple add-on module into existing text watermarking technologies, seamlessly transforming them into multimodal watermarking content systems without compromising their original usability and user experience. Our contributions can be summarized as follows:

- This paper proposes an innovative multimodal watermarking framework that enables seamless conversion between text and image watermark content, effectively bridging the gap between text watermarking and image steganography technologies for the first time.
- The framework incorporates an innovative image feature restoration module, which significantly enhances the robustness of watermark content during transmission and ensures the integrity of its conversion into image content, even under various noise and interference conditions
- The multimodal watermarking module can be seamlessly integrated into existing text watermarking technologies, transforming them into multimodal watermark content models without compromising the original user experience or functionality.
- Comprehensive experiments focusing on the robustness of the watermark demonstrate the superiority and stability of the proposed method compared to existing approaches.

## 2. Related Work

### 2.1. Diffusion Models

Diffusion models [Nichol and Dhariwal \(2021\)](#)[Song and Ermon \(2019\)](#)[Song et al. \(2020\)](#) are a class of emerging deep generative models that have demonstrated groundbreaking performance in various applications, such as image synthesis [Dhariwal and Nichol \(2021\)](#)[Saharia et al. \(2022a\)](#)[Ramesh et al. \(2022\)](#), video generation [Ho et al. \(2022a\)](#)[Ho et al. \(2022b\)](#), and image restoration [Saharia et al. \(2022b\)](#)[Wang et al. \(2023\)](#)[Kawar et al. \(2022\)](#). The core principle of these models is to simulate the physical diffusion process: noise is incrementally added to the data, transforming it into a noisy state, which can then be reconstructed back to its original form through a reverse process. Initially, [Ho et al. \(2020\)](#) introduced the denoising diffusion probabilistic model (DDPM), which laid the groundwork for subsequent research [Lyu et al. \(2019\)](#)[Gu et al. \(2022\)](#)[Lu et al. \(2022\)](#). Later, [Rombach et al. \(2022\)](#) proposed latent diffusion models, significantly reducing computational complexity and improving efficiency, thus further advancing the development of diffusion models [Kim et al. \(2022\)](#)[Meng et al. \(2021\)](#)[Tang et al. \(2023\)](#). This progress has spurred a wave of innovation within the diffusion model community, leading to many new approaches. [Gandikota et al. \(2023\)](#)[Wang et al. \(2024\)](#) In this paper, our proposed framework also leverages diffusion-based watermarking techniques, harnessing

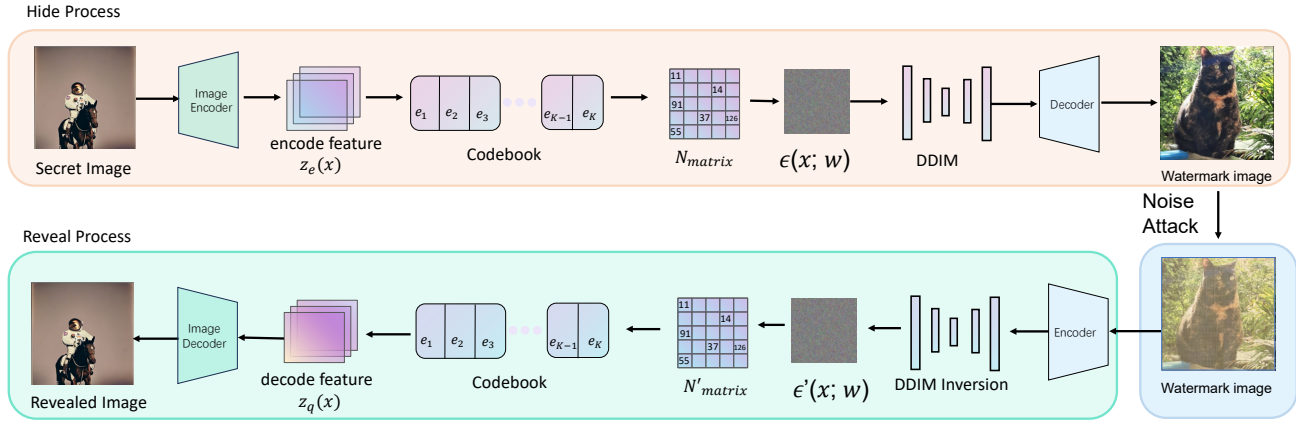


Figure 3. This figure describes in detail the overall framework of the multi-modal watermarking content method proposed in this paper. First, the input image  $x$  is converted into a high-dimensional latent feature representation  $z_e(x)$  through a multi-layer convolutional encoder. After that, these features are converted into a binary watermark by forming an adjacency matrix  $N_{matrix}$  through codebook mapping and quantization, and then embedded into the latent features through a diffusion model. Through the restoration and decoding process, the model finally generates an image containing the watermark information, ensuring the concealment of the watermark and its robustness to attacks.

their inherent robustness and security benefits to strengthen our multi-modal watermarking method.

## 2.2. Image Watermarking

Image-text watermarking technology [Ahmadi et al. \(2020\)](#)[Liu et al. \(2024\)](#), as a means of embedding textual information within images, is primarily used to insert copyright details, authentication data, or other sensitive text for tracking, verification, and copyright protection purposes. Huang et al. [Huang et al. \(2019\)](#) proposed an adaptive image watermarking method that can be directly applied to the outputs of diffusion models. Zhu et al. [Zhu et al. \(2018\)](#) introduced a watermark embedding approach based on adversarial training. these methods effectively enhance the robustness and imperceptibility of the watermark, but like other post-processing techniques, it can still significantly affect image quality. Recent approaches, such as the Stable Signature method [Fernandez et al. \(2023\)](#) and the method proposed by Zhao et al. [Zhao et al. \(2023\)](#), attempt to embed watermarks during the diffusion generation process to mitigate impacts on image quality. However, these methods only allow the extraction of fixed watermark information. Other innovative studies, such as the Tree-ring method [Wen et al. \(2023\)](#), aim to embed copyright information by modifying latent representations, thereby eliminating training costs; however, this approach only achieves copyright protection without enabling the transmission of meaningful information. Even the latest models, such as Gaussian Shading [Yang et al. \(2024\)](#), are limited to transmitting approximately 512 bits of effective information. Consequently, the bit limitations of image-text watermarks restrict the density

of content they can carry.

## 2.3. Steganography Methods

Image steganography is a technique for embedding secret information into a host image, aiming to create an information carrier that is difficult to detect. For instance, Zhu et al. [Zhu et al. \(2018\)](#) and Zhang et al. [Zhang et al. \(2019\)](#) attempted to introduce adversarial learning methods, utilizing an encode-decode architecture to automatically learn the embedding and recovery of information, in order to explore the balance between image quality and image steganography. In references [Lu et al. \(2021\)](#) and [Jing et al. \(2021\)](#), researchers proposed an innovative design for steganographic models by constructing them as invertible neural networks (INN) [Dinh et al. \(2014\)](#)[Dinh et al. \(2016\)](#). Building on this, coverless steganography is an emerging approach that does not modify the host object, making it more challenging for attackers to detect hidden data. Examples of this approach include the techniques found in [Luo et al. \(2020\)](#) and [Zou et al. \(2022\)](#), which have emerged as notable methods within the field. Currently, researchers are exploring steganography methods that do not rely on host images, aiming to achieve even higher security in communication. However, most existing methods still depend on embedding data into carrier images, which means that perturbation attacks on these images can significantly impact the hidden content.

### 3. Methods

#### 3.1. Application Scenarios

As show in Figure 2, the proposed multi-modal watermarking content method has been validated for its effectiveness across multiple application scenarios. The scenarios involve three models: Image-Watermark Model A, Image Steganography Model B, and the proposed Multi-modal Watermarking Model C. Users Judy and Hence, along with an attacker Martin, tested these models. Judy attempted to embed a copyright mark using Models A and B but found them ineffective under attack. In contrast, Hence successfully embedded a robust watermark using Model C. Even after the attack, the watermark remained intact, proving ownership and demonstrating the robustness of the multi-modal approach.

#### 3.2. Seamless Text-Image Watermarking

This section introduces an innovative multi-modal watermarking technique aimed at enabling seamless conversion between text and image watermarks. This method first constructs a codebook to vectorize the image to be embedded, then applies vector quantization to map the image features onto a predefined codebook. Next, an adjacency matrix is generated based on the similarity of discrete vectors, encoding the structural information of the image as binary data to achieve seamless conversion between text and image. Section 3.2.1 presents a mathematical proof of the vector discretization encoding, and introduce its specific application within this method in subsequent chapters.

##### 3.2.1. Foundations of Discrete Encoding

**Encoding:** For an input image, the model extracts key information via a deep neural network, transforming it into a continuous latent representation.

**CodeBook:** A codebook is a finite set of vectors (code-words) representing the discrete latent space of the input. These pre-learned vectors act as a "vocabulary," mapping image features to discrete codebook vectors during vector quantization, transitioning from continuous to discrete latent space.

**Decoding:** The selected codebook vector reconstructs or represents the original input.

The mathematical expression of vector quantization can be defined as follows:

**Encoder Output:** Let  $z_e(x)$  be the encoder's continuous latent representation for input  $x$ .

**Vector Quantization Layer:** This layer maps  $z_e(x)$  to a discrete latent space by finding the closest vector  $e_k$  in the codebook  $\{e_1, e_2, \dots, e_K\}$ , where  $K$  is the codebook size:

$$z_q(x) = \operatorname{argmin}_k \|z_e(x) - e_k\|_2^2 \quad (1)$$

where  $\|\cdot\|_2$  denotes the L2 norm (Euclidean distance).

**Embedding Loss:** The embedding loss  $L$  combines the distance between the encoder output and the quantized vector, and the distance between the quantized vector (via embedding network  $g$ ) and the encoder output:

$$L = \mathbb{E}_{x, z_e(x), z_q(x)} [\|z_e(x) - z_q(x)\|_2^2] + \beta \mathbb{E}_{x, z_q(x)} [\|z_e(x) - g(z_q(x))\|_2^2] \quad (2)$$

Here,  $g$  is the embedding network, and  $\beta$  balances the two terms. The first term is the vector quantization loss ( $L_{\text{embedding}}$ ), while the second is the commitment loss ( $L_{\text{commitment}}$ ), ensuring the encoder commits to the selected codebook vector and stabilizes training. Together, these terms maintain discrete encoder outputs while optimizing image quality.



Figure 4. The image watermark imaging effect of the multi-modal watermarking method under attack conditions without image restoration module.

#### 3.3. Multi-Modal Watermarking Method

The proposed method utilizes codebook and feature discretization techniques to achieve text-to-image pair conversion. Considering the training overhead and watermark capacity, we selected the Gaussian Shading model as the foundational model within the proposed multi-modal watermarking framework. In summary, the multi-modal watermark framework of this paper is shown in Figure 3.

During watermark embedding, the input image  $x$  is first transformed into high-dimensional latent features  $z_e(x)$  using a multi-layer convolutional encoder. These features are then quantized into discrete codewords via a codebook, forming an adjacency matrix  $N_{\text{matrix}}$ . The matrix is constructed by computing pairwise cosine similarities between latent feature vectors:

$$N_{\text{matrix}}(i, j) = \frac{z_e(x)_i \cdot z_e(x)_j}{\|z_e(x)_i\|_2 \|z_e(x)_j\|_2} \quad (3)$$

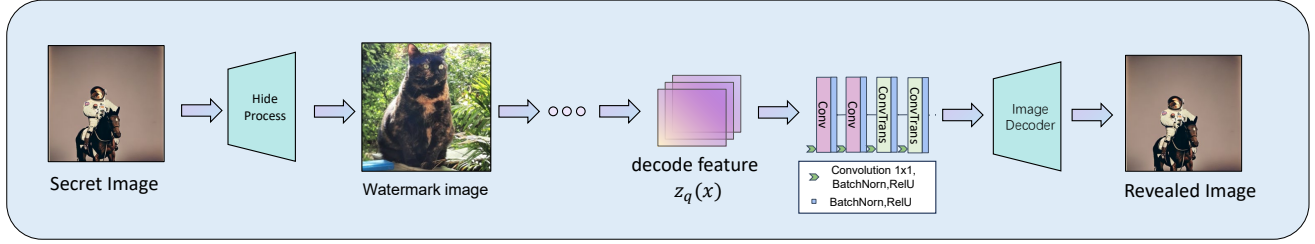


Figure 5. The architecture of the image restoration module. This module removes lossy stain blocks by compressing features and restores image features through upsampling technology, thereby effectively ensuring the imaging effect of the image.

where  $z_e(x)_i$  and  $z_e(x)_j$  are latent feature vectors, and  $N_{\text{matrix}}(i, j)$  represents the element at the  $i$ -th row and  $j$ -th column of the adjacency matrix.

Next, the adjacency matrix  $N_{\text{matrix}}$  is converted into a binary secret watermark. First, the matrix is resized to a  $16 \times 16$  dimension to match the required binary watermark length, considering the capacity of the text watermark. Then, each element of the adjacency matrix is transformed into an 8-bit binary representation, and these binary strings are concatenated to form the final binary watermark. This process can be expressed as:

$$w = \text{Concatenate}(\text{Binary}(N_{\text{matrix}}(i, j), 8)) \quad (4)$$

where  $\text{Binary}(N_{\text{matrix}}(i, j), 8)$  denotes the conversion of each adjacency matrix element into an 8-bit binary string, and  $\text{Concatenate}$  signifies the joining of these binary strings to form the binary watermark  $w$ .

Subsequently, the binary watermark information is input into a diffusion model, projecting the watermark information onto the latent feature representation using Gaussian shading technology. This process adheres to the standard Gaussian distribution, ensuring the stealth of the watermark, which can be represented as:

$$z_w = z_e(x) + \eta \quad (5)$$

where  $\eta$  is Gaussian noise, and  $z_w$  is the latent feature representation containing the watermark information.

Finally, through the restoration module of the diffusion model, the latent feature representation containing the watermark information is converted back into the image space, ultimately generating a watermarked image through the decoder. The decoder utilizes its complex network structure, including transposed convolutional layers and activation functions, to map the latent features back into the original image space.

In our proposed method, we also carefully designed the training loss functions. We observed that relying solely on reconstruction loss can result in overly smooth generated images, leading to a loss of crucial texture details. Therefore, we incorporated a perceptual loss function to better

preserve the image’s fine details and textures. The perceptual loss leverages a pre-trained deep neural network (such as the VGG network) to extract feature representations of the image and compare the differences in these feature layers. The perceptual loss can be defined as:

$$L_{\text{perceptual}} = \|f_k(I_{\text{real}}) - f_k(I_{\text{fake}})\|_1 \quad (6)$$

where  $I_{\text{real}}$  represents the real image,  $I_{\text{fake}}$  is the generated image,  $f_k$  denotes the feature extraction function at the  $k$ -th layer of the pre-trained deep network, and  $\|\cdot\|_1$  indicates the L1 norm, used to compute the absolute difference between two feature maps.

The total loss function for our model combines perceptual loss, vector quantization loss, and commitment loss as a weighted sum, represented as:

$$L_{\text{total}} = L_{\text{perceptual}} + \alpha L_{\text{embedding}} + \beta L_{\text{commitment}} \quad (7)$$

where  $\alpha$  and  $\beta$  are hyperparameters balancing the contributions of each loss term. With this loss function design, our model optimizes the quality and diversity of generated images while maintaining the discreteness of the encoder outputs, ensuring that the generated images retain high visual quality and rich texture details.

### 3.4. More Robust Multi-Modal Watermarking Method

We address the robustness of text watermarks under severe attacks and design a more resilient watermarking method. Text watermarks may be compromised during transmission, making it difficult to ensure 100% accuracy, which directly impacts image watermarks, as shown in Figure 4. This raises a key challenge: how to maintain image quality when text watermarks are damaged during transmission.

To address this challenge, we introduce an image restoration module, as illustrated in Figure 5. This module removes feature impurities through feature compression and restores clean features using upsampling techniques, thereby effectively preserving image quality. Specifically, the module compresses and upsamples feature maps to repair and enhance damaged features, ensuring visual quality

| methods  | clean | Grussian noise |              |              | Brightness   |              |              | Random Crop  |              |              |
|--|-------|----------------|--------------|--------------|--------------|--------------|--------------|--------------|--------------|--------------|
|  |       | $\theta=0.05$  | $\theta=0.1$ | $\theta=0.2$ | $\theta=1$   | $\theta=2$   | $\theta=4$   | $\theta=0.2$ | $\theta=0.4$ | $\theta=0.8$ |
| Baluja (256) <a href="#">Baluja (2019)</a>     | 28.91 | 9.52           | 9.48         | 9.32         | 8.90         | 7.30         | 6.00         | 9.33         | 9.21         | 9.00         |
| Baluja (512) <a href="#">Baluja (2019)</a>     | 28.79 | 9.54           | 9.50         | 9.33         | 9.55         | 7.31         | 6.00         | 9.27         | 9.08         | 8.72         |
| HiNet (256) <a href="#">Jing et al. (2021)</a> | 33.37 | 7.81           | 6.51         | 6.13         | <b>23.73</b> | 18.49        | 16.74        | 10.78        | 11.13        | 12.73        |
| HiNet (512) <a href="#">Jing et al. (2021)</a> | 33.93 | 6.90           | 5.49         | 5.01         | 21.71        | 18.56        | 15.86        | 10.72        | 11.23        | 14.28        |
| CRoSS (256) <a href="#">Yu et al. (2024)</a>   | 15.62 | 11.50          | 10.75        | 9.61         | 13.09        | 11.11        | 10.59        | 6.43         | 6.84         | 9.59         |
| CRoSS (512) <a href="#">Yu et al. (2024)</a>   | 25.30 | 17.04          | 14.57        | 11.61        | 17.70        | 14.69        | 12.54        | 6.32         | 6.97         | 10.61        |
| RoSMM-w  | 22.21 | 12.00          | 10.14        | 9.38         | 20.03        | 19.48        | 17.04        | 9.24         | 9.33         | 13.75        |
| RoSMM(ours)                                    | 20.35 | <b>17.32</b>   | <b>15.23</b> | <b>12.28</b> | 20.70        | <b>20.69</b> | <b>19.90</b> | <b>10.92</b> | <b>11.23</b> | <b>18.69</b> |

Table 1. The PSNR (dB) performance results of different methods under various types of attacks. The higher the PSNR value, the better the image quality.

| methods      | clean | Gaussian noise |              | Brightness   |              |
|--------------|-------|----------------|--------------|--------------|--------------|
|              |       | $\theta=0.1$   | $\theta=0.2$ | $\theta=1$   | $\theta=2$   |
| Baluja (256) | 0.934 | 0.132          | 0.069        | 0.260        | 0.253        |
| Baluja (512) | 0.920 | 0.162          | 0.074        | 0.386        | 0.375        |
| HiNet (256)  | 0.930 | 0.014          | 0.005        | 0.576        | 0.505        |
| HiNet (512)  | 0.933 | 0.006          | 0.005        | 0.580        | 0.545        |
| CRoSS (256)  | 0.364 | 0.171          | 0.133        | 0.290        | 0.281        |
| CRoSS (512)  | 0.853 | 0.230          | 0.117        | 0.578        | 0.546        |
| RoSMM-w      | 0.636 | 0.222          | 0.199        | 0.586        | 0.505        |
| RoSMM(ours)  | 0.615 | <b>0.439</b>   | <b>0.366</b> | <b>0.598</b> | <b>0.581</b> |

Table 2. The SSIM performance results of different methods under various types of attacks. The closer the SSIM value is to 1, the better the image quality.

even when watermark information is compromised. Figure 6 compares the watermarking results with and without the restoration module, demonstrating its effectiveness in enhancing robustness and readability under damaged transmission conditions.

More specifically, The image restoration module employs an encode-decode structure with multiple downsampling and upsampling operations. The encoder consists of three downsampling blocks, each including a  $3 \times 3$  convolutional layer, batch normalization, and ReLU activation, compressing features to form watermark encodings. The decoder, symmetric to the encoder, includes multiple upsampling blocks with  $3 \times 3$  transposed convolutional layers, batch normalization, and ReLU activation. Skip connections are introduced in the initial downsampling stage to enhance high-frequency information recovery, ensuring clear watermark identification even under damaged transmission.

In summary, the proposed multi-modal watermarking framework is theoretically innovative and demonstrates ex-

cellent performance in practical applications. By integrating perceptual loss, an image restoration module, and multi-modal watermarking techniques, our framework effectively resists various attacks during watermark transmission, ensuring the robustness of the watermark while maintaining the integrity of the image watermark content restored from the text watermark.

## 4. Experiment

### 4.1. Implementation Details

**Experimental Settings** In this paper, we selected Stable Diffusion v2.1 [Rombach et al. \(2022\)](#) as the conditional diffusion model, and implemented the Gaussian Shading model [Yang et al. \(2024\)](#) for text watermarking within our multi-modal watermarking method. According to the specifications of the Gaussian Shading model [Yang et al. \(2024\)](#), we configured the hyperparameters as follows:  $fh = 2$ ,  $fc = 2$ , and  $l = 1$  and setting the binary watermark capacity at 2048 bits. For seamless text-to-image transformation, we defined the adjacency matrix size as  $16 \times 16$ , and set the embedding depth of the codebook to 512 with a length of 256, allowing each codeword to be converted into an 8-bit binary encoding for efficient embedding in the text watermarking model, and the RoSMM-w means the RoSMM model without feature restoration module. All experiments were conducted on an A6000 GPU, and our approach required no additional training or fine-tuning of the diffusion model, only the image-to-text and text-to-image transformation modules were trained. In addition, we have not identified any method that simultaneously achieves image steganography and text content watermarking. For comparison, we selected HiNet [Jing et al. \(2021\)](#), Baluja [Baluja \(2019\)](#) as a classic traditional image steganography method, and compared it with the latest diffusion-based image steganography method CRoSS [Yu et al. \(2024\)](#), demonstrating the robustness and readability of this method in im-

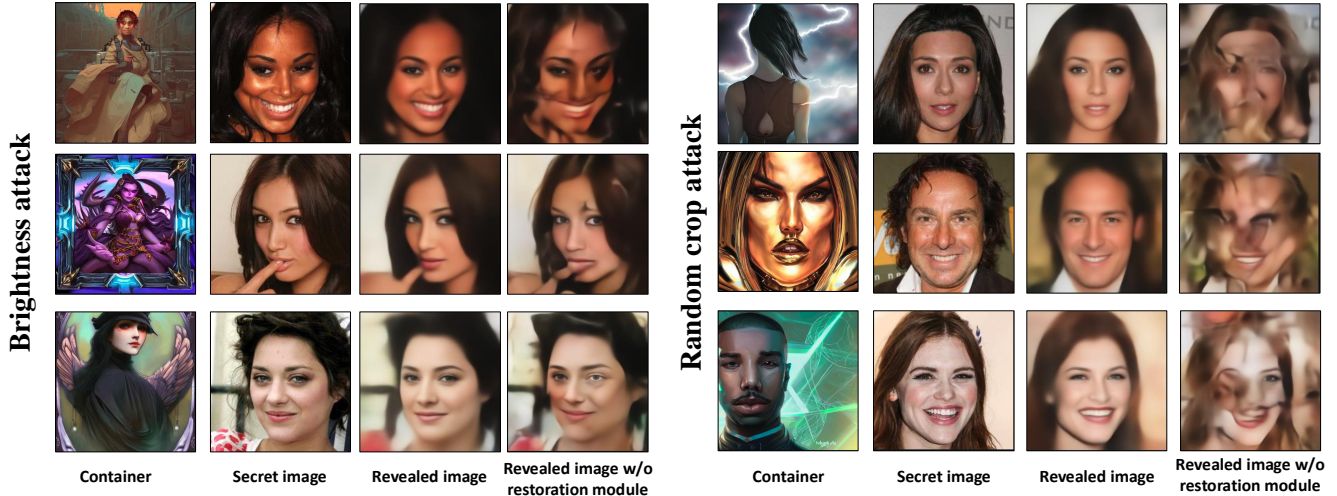


Figure 6. This figure compares the watermark imaging effects of the model under lossy transmission conditions with and without the image restoration module. The left column displays the watermark images without the restoration module, while the right column shows the imaging results after the introduction of the image restoration module.

age generation quality.

**Data Preparation** Regarding datasets, we selected CelebA-HQ [Karras \(2017\)](#) as our benchmark dataset. This dataset was generated by training a high-resolution Generative Adversarial Network (GAN) based on the original CelebA dataset [Liu et al. \(2015\)](#). It contains a total of 30,000 images, each available in multiple resolutions, ranging from 64x64 to 1024x1024 pixels. Due to its high quality and diversity, CelebA-HQ is widely used across various computer vision domains, including object detection, image generation, and facial recognition. In this experiment, we randomly selected 100 images as our test set, with the remaining data used for training.

## 4.2. Comparison to Baselines

In the experimental section, we examine various attack scenarios to evaluate the robustness of our proposed method in real-world applications. Specifically, we subjected container images embedded with secret images to several types of attack, including Random Crop, Gaussian noise, and Brightness attack. The hyperparameters  $\theta$  represent the varying intensities of the aforementioned attacks. Following each attack, we extracted the secret image from the container to assess the robustness of watermark transmission.

To reduce the capacity load on text watermark transmission, our method RoSMM generates watermark images with a resolution of  $256 \times 256$ . We used PSNR (Peak Signal-to-Noise Ratio) and SSIM (Structural Similarity Index) as metrics to evaluate the robustness of other algorithms in watermarking at different image scales, where PSNR is used to quantify the loss of image quality, and SSIM is used to measure the structural similarity of images.

As shown in [Table 1](#) and [Table 2](#), compared to other methods, our multi-modal watermarking architecture demonstrates excellent robustness under multiple attack conditions.

In most attack scenarios, our method achieves the best performance. Only when the brightness attack strength is 0.5, HiNet [Jing et al. \(2021\)](#) outperforms our method. One possible reason is that when  $\theta = 0.5$ , the attack has less impact on the watermark, making it difficult for other methods to surpass HiNet [Jing et al. \(2021\)](#) in image quality. However, even under this brightness attack, our method showed only slight performance degradation, whereas HiNet’s [Jing et al. \(2021\)](#) PSNR dropped sharply from 33.37 db to 23.73 db, reducing image quality by approximately 30%, and Baluja [Baluja \(2019\)](#) PSNR dropped from 28.91 db to 8.90 db. Meanwhile, CRoSS [Yu et al. \(2024\)](#) exhibited less fluctuation in performance, highlighting the advantages of diffusion models in image steganography. However, under high-intensity attacks, its PSNR and SSIM metrics remain slightly lower than our method, and in the case of Gaussian noise attacks, when  $\theta = 0.2$ , its SSIM value drops to 0.005, while ours remains around 0.366.

Unlike traditional image steganography methods, our proposed multi-modal method, RoSMM, leverages the advantages of text watermarking to demonstrate superior robustness in watermark transmission. This method effectively combines the strengths of image and text watermarking, enabling the model to successfully transmit image watermark information with rich content through text watermarks.

| methods                             | clean | Gaussian noise |              |              | brightness   |             |             | Random Crop  |              |              |
|-------------------------------------|-------|----------------|--------------|--------------|--------------|-------------|-------------|--------------|--------------|--------------|
|                                     |       | $\theta=0.05$  | $\theta=0.1$ | $\theta=0.2$ | $\theta=0.5$ | $\theta=1$  | $\theta=2$  | $\theta=0.2$ | $\theta=0.4$ | $\theta=0.8$ |
| Gaussian Shading Yang et al. (2024) | 99.2  | 83.2           | 72.8         | 63.5         | <b>99.0</b>  | <b>98.4</b> | <b>95.0</b> | 58.0         | 71.6         | 89.9         |
| RoSMM(ours)                         | 96.8  | <b>84.0</b>    | <b>75.8</b>  | <b>71.7</b>  | 95.0         | 94.8        | 94.2        | <b>69.8</b>  | <b>72.2</b>  | <b>90.1</b>  |

Table 3. Accurate(%) results of the impact of image watermark robustness on text watermark Performance.

### 4.3. Internal Robustness Analysis of Multi-Modal Watermarks

In this section, we explore the impact of image watermarking and text watermarking technologies within the multi-modal watermarking framework and draw conclusions through experimental analysis. The framework does not simply concatenate image and text watermarks but instead creates a novel structure to integrate these technologies, fully leveraging their respective strengths and enabling mutual influence, thereby effectively harnessing the advantages of both text and image watermarking.

The Gaussian Shading model Yang et al. (2024), serving as the base for the text watermarking algorithm, offers strong robustness and can transmit over 512 bits of data. As shown in Table 3, the Gaussian Shading model Yang et al. (2024) maintains over 90% accuracy under various attacks, highlighting its potential in real-world scenarios. However, its accuracy drops significantly under extreme conditions like Random Crop and Gaussian noise, falling to 58% at  $\theta=0.2$  for Random Crop, indicating limitations in text watermarking.

To address this, we innovatively reframe text watermark repair as an image feature restoration problem. By improving image watermark quality, we indirectly enhance text watermark accuracy. As shown in Table 1, without the image restoration module, RoSMM-w exhibits lower image quality compared to RoSMM, dropping from 12.28 dB to 9.38 dB under Gaussian noise at  $\theta=0.2$ . This confirms the effectiveness of the image feature restoration module in enhancing watermark robustness. Additionally, Table 3 shows that improving image quality positively impacts watermark accuracy, especially when the initial accuracy is low. For example, under Random Crop at  $\theta=0.2$ , text watermark accuracy increases from 58.0% to 69.8% after image restoration. This improvement continues until the text watermark accuracy reaches 96% or higher. As shown in Figure 7, we conducted ablation experiments by testing the proposed method with various attack intensities to evaluate whether the image restoration module can effectively improve the accuracy of text watermarking. The results demonstrate that, in the vast majority of cases under attack interference, the proposed method can adapt to almost all attack methods, and the text watermark accuracy of RoSMM consistently outperforms that of the baseline methods.

The proposed multi-modal watermarking content method achieves the synergy between image watermarking and text watermarking. Text watermarking ensures the robust transmission of image content, while image watermarking technology, in turn, provides the potential to enhance the transmission accuracy of text watermarks.

## 5. Conclusion

In this paper, we propose a multi-modal watermarking framework by integrating text content watermarking and image content watermarking into a unified system, introducing a novel multi-modal watermarking content method. This method leverages vector discretization in encoder-based vector quantization to achieve mutual transformation between text content watermarks and image content watermarks, addressing a key limitation in existing technologies. The inclusion of a restoration module effectively mitigates accuracy loss caused by various attacks, significantly enhancing the robustness of the watermark while maintaining the integrity of the image content. Experimental results demonstrate that the method exhibits strong resistance to almost all noise attacks, making it a secure and scalable solution for digital copyright protection.

## References

- Mahdi Ahmadi, Alireza Norouzi, Nader Karimi, Shadrokh Samavi, and Ali Emami. Redmark: Framework for residual diffusion watermarking based on deep networks. *Expert Systems with Applications*, 146:113157, 2020. 3
- Vishal Asnani, John Collomosse, Tu Bui, Xiaoming Liu, and Shruti Agarwal. Promark: Proactive diffusion watermarking for causal attribution. In *Proceedings of the IEEE/CVF Conference on Computer Vision and Pattern Recognition*, pages 10802–10811, 2024. 1
- Shumeet Baluja. Hiding images within images. *IEEE transactions on pattern analysis and machine intelligence*, 42(7):1685–1697, 2019. 6, 7
- Hai Ci, Yiren Song, Pei Yang, Jinheng Xie, and Mike Zheng Shou. Wmadapter: Adding watermark control to latent diffusion models. *arXiv preprint arXiv:2406.08337*, 2024. 1
- Prafulla Dhariwal and Alexander Nichol. Diffusion models beat gans on image synthesis. *Advances in neural information processing systems*, 34:8780–8794, 2021. 2
- Laurent Dinh, David Krueger, and Yoshua Bengio. Nice: Non-

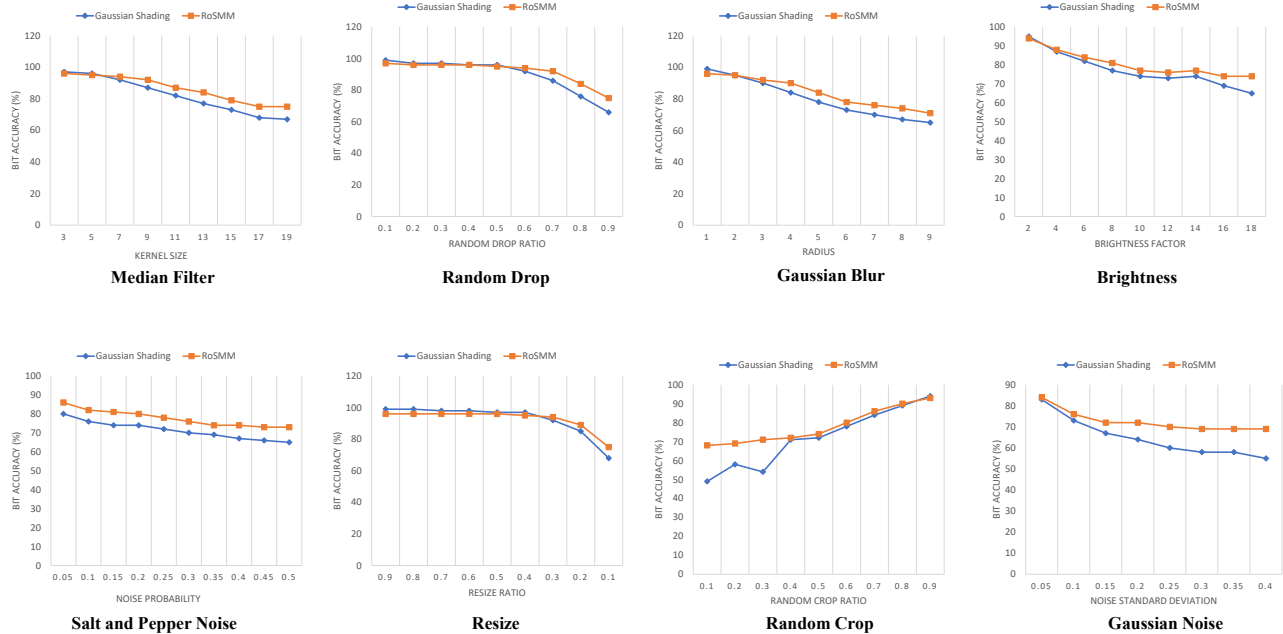


Figure 7. Perturbation Attack Results: We conducted ablation experiments on the proposed model with varying noise intensities

linear independent components estimation. *arXiv preprint arXiv:1410.8516*, 2014. 3

Laurent Dinh, Jascha Sohl-Dickstein, and Samy Bengio. Density estimation using real nvp. *arXiv preprint arXiv:1605.08803*, 2016. 3

Pierre Fernandez, Guillaume Couairon, Hervé Jégou, Matthijs Douze, and Teddy Furon. The stable signature: Rooting watermarks in latent diffusion models. In *Proceedings of the IEEE/CVF International Conference on Computer Vision*, pages 22466–22477, 2023. 1, 3

Rohit Gandikota, Joanna Materzynska, Jaden Fiotto-Kaufman, and David Bau. Erasing concepts from diffusion models. In *Proceedings of the IEEE/CVF International Conference on Computer Vision*, pages 2426–2436, 2023. 2

Shuyang Gu, Dong Chen, Jianmin Bao, Fang Wen, Bo Zhang, Dongdong Chen, Lu Yuan, and Baining Guo. Vector quantized diffusion model for text-to-image synthesis. In *Proceedings of the IEEE/CVF conference on computer vision and pattern recognition*, pages 10696–10706, 2022. 2

Jonathan Ho, Ajay Jain, and Pieter Abbeel. Denoising diffusion probabilistic models. *Advances in neural information processing systems*, 33:6840–6851, 2020. 2

Jonathan Ho, William Chan, Chitwan Saharia, Jay Whang, Ruiqi Gao, Alexey Gritsenko, Diederik P Kingma, Ben Poole, Mohammad Norouzi, David J Fleet, et al. Imagen video: High definition video generation with diffusion models. *arXiv preprint arXiv:2210.02303*, 2022a. 2

Jonathan Ho, Tim Salimans, Alexey Gritsenko, William Chan, Mohammad Norouzi, and David J Fleet. Video diffusion models. *Advances in Neural Information Processing Systems*, 35: 8633–8646, 2022b. 2

Ying Huang, Baoning Niu, Hu Guan, and Shuwu Zhang. Enhancing image watermarking with adaptive embedding parameter and psnr guarantee. *IEEE Transactions on Multimedia*, 21(10): 2447–2460, 2019. 3

Priyank Jaini, Kira A Selby, and Yaoliang Yu. Sum-of-squares polynomial flow. In *International Conference on Machine Learning*, pages 3009–3018. PMLR, 2019. 2

Junpeng Jing, Xin Deng, Mai Xu, Jianyi Wang, and Zhenyu Guan. Hinet: Deep image hiding by invertible network. In *Proceedings of the IEEE/CVF international conference on computer vision*, pages 4733–4742, 2021. 1, 3, 6, 7

Tero Karras. Progressive growing of gans for improved quality, stability, and variation. *arXiv preprint arXiv:1710.10196*, 2017. 7

Bahjat Kawar, Michael Elad, Stefano Ermon, and Jiaming Song. Denoising diffusion restoration models. *Advances in Neural Information Processing Systems*, 35:23593–23606, 2022. 2

Gwanghyun Kim, Taesung Kwon, and Jong Chul Ye. Diffusion-clip: Text-guided diffusion models for robust image manipulation. In *Proceedings of the IEEE/CVF conference on computer vision and pattern recognition*, pages 2426–2435, 2022. 2

Guan-Hong Liu, Tianrong Chen, Evangelos Theodorou, and Molei Tao. Mirror diffusion models for constrained and watermarked generation. *Advances in Neural Information Processing Systems*, 36, 2024. 3

Ziwei Liu, Ping Luo, Xiaogang Wang, and Xiaoou Tang. Deep learning face attributes in the wild. In *Proceedings of International Conference on Computer Vision (ICCV)*, 2015. 7

Cheng Lu, Yuhao Zhou, Fan Bao, Jianfei Chen, Chongxuan Li, and Jun Zhu. Dpm-solver: A fast ode solver for diffusion probabilistic model sampling in around 10 steps. *Advances in Neural Information Processing Systems*, 35:5775–5787, 2022. 2

- Shao-Ping Lu, Rong Wang, Tao Zhong, and Paul L Rosin. Large-capacity image steganography based on invertible neural networks. In *Proceedings of the IEEE/CVF conference on computer vision and pattern recognition*, pages 10816–10825, 2021. 1, 3
- Yuanjing Luo, Jiaohua Qin, Xuyu Xiang, and Yun Tan. Coverless image steganography based on multi-object recognition. *IEEE Transactions on Circuits and Systems for Video Technology*, 31(7):2779–2791, 2020. 3
- He Lyu, Ningyu Sha, Shuyang Qin, Ming Yan, Yuying Xie, and Rongrong Wang. Advances in neural information processing systems. *Advances in neural information processing systems*, 32, 2019. 2
- Chenlin Meng, Yutong He, Yang Song, Jiaming Song, Jiajun Wu, Jun-Yan Zhu, and Stefano Ermon. Sedit: Guided image synthesis and editing with stochastic differential equations. *arXiv preprint arXiv:2108.01073*, 2021. 2
- Alexander Quinn Nichol and Prafulla Dhariwal. Improved denoising diffusion probabilistic models. In *International conference on machine learning*, pages 8162–8171. PMLR, 2021. 1, 2
- Kushagra Pandey, Avideep Mukherjee, Piyush Rai, and Abhishek Kumar. Diffusevae: Efficient, controllable and high-fidelity generation from low-dimensional latents. *arXiv preprint arXiv:2201.00308*, 2022. 1
- George Papamakarios, Theo Pavlakou, and Iain Murray. Masked autoregressive flow for density estimation. *Advances in neural information processing systems*, 30, 2017. 2
- Aditya Ramesh, Prafulla Dhariwal, Alex Nichol, Casey Chu, and Mark Chen. Hierarchical text-conditional image generation with clip latents. *arXiv preprint arXiv:2204.06125*, 1(2):3, 2022. 2
- Robin Rombach, Andreas Blattmann, Dominik Lorenz, Patrick Esser, and Björn Ommer. High-resolution image synthesis with latent diffusion models. In *Proceedings of the IEEE/CVF conference on computer vision and pattern recognition*, pages 10684–10695, 2022. 1, 2, 6
- Chitwan Saharia, William Chan, Saurabh Saxena, Lala Li, Jay Whang, Emily L Denton, Kamyar Ghasemipour, Raphael Gontijo Lopes, Burcu Karagol Ayan, Tim Salimans, et al. Photorealistic text-to-image diffusion models with deep language understanding. *Advances in neural information processing systems*, 35:36479–36494, 2022a. 2
- Chitwan Saharia, Jonathan Ho, William Chan, Tim Salimans, David J Fleet, and Mohammad Norouzi. Image super-resolution via iterative refinement. *IEEE transactions on pattern analysis and machine intelligence*, 45(4):4713–4726, 2022b. 2
- Yang Song and Stefano Ermon. Generative modeling by estimating gradients of the data distribution. *Advances in neural information processing systems*, 32, 2019. 2
- Yang Song, Jascha Sohl-Dickstein, Diederik P Kingma, Abhishek Kumar, Stefano Ermon, and Ben Poole. Score-based generative modeling through stochastic differential equations. *arXiv preprint arXiv:2011.13456*, 2020. 2
- Luming Tang, Menglin Jia, Qianqian Wang, Cheng Perng Phoo, and Bharath Hariharan. Emergent correspondence from image diffusion. *Advances in Neural Information Processing Systems*, 36:1363–1389, 2023. 2
- Bram Wallace, Akash Gokul, and Nikhil Naik. Edict: Exact diffusion inversion via coupled transformations. In *Proceedings of the IEEE/CVF Conference on Computer Vision and Pattern Recognition*, pages 22532–22541, 2023. 1
- Yinhuai Wang, Jiwen Yu, and Jian Zhang. Zero-shot image restoration using denoising diffusion null-space model. *The Eleventh International Conference on Learning Representations*, 2023. 2
- Zhendong Wang, Yifan Jiang, Huangjie Zheng, Peihao Wang, Pengcheng He, Zhangyang Wang, Weizhu Chen, Mingyuan Zhou, et al. Patch diffusion: Faster and more data-efficient training of diffusion models. *Advances in neural information processing systems*, 36, 2024. 2
- Daniel Watson, William Chan, Jonathan Ho, and Mohammad Norouzi. Learning fast samplers for diffusion models by differentiating through sample quality. In *International Conference on Learning Representations*, 2022. 1
- Yuxin Wen, John Kirchenbauer, Jonas Geiping, and Tom Goldstein. Tree-ring watermarks: Fingerprints for diffusion images that are invisible and robust. *arXiv preprint arXiv:2305.20030*, 2023. 3
- Yuxin Wen, John Kirchenbauer, Jonas Geiping, and Tom Goldstein. Tree-rings watermarks: Invisible fingerprints for diffusion images. *Advances in Neural Information Processing Systems*, 36, 2024. 1
- Cheng Xiong, Chuan Qin, Guorui Feng, and Xinpeng Zhang. Flexible and secure watermarking for latent diffusion model. In *Proceedings of the 31st ACM International Conference on Multimedia*, pages 1668–1676, 2023. 1
- Zijin Yang, Kai Zeng, Kejiang Chen, Han Fang, Weiming Zhang, and Nenghai Yu. Gaussian shading: Provable performance-lossless image watermarking for diffusion models. In *Proceedings of the IEEE/CVF Conference on Computer Vision and Pattern Recognition*, pages 12162–12171, 2024. 1, 3, 6, 8
- Jiwen Yu, Xuanyu Zhang, Youmin Xu, and Jian Zhang. Cross: Diffusion model makes controllable, robust and secure image steganography. *Advances in Neural Information Processing Systems*, 36, 2024. 6, 7
- Kevin Alex Zhang, Alfredo Cuesta-Infante, Lei Xu, and Kalyan Veeramachaneni. Steganogan: High capacity image steganography with gans. *arXiv preprint arXiv:1901.03892*, 2019. 3
- Yunqing Zhao, Tianyu Pang, Chao Du, Xiao Yang, Ngai-Man Cheung, and Min Lin. A recipe for watermarking diffusion models. *arXiv preprint arXiv:2303.10137*, 2023. 3
- Jiren Zhu, Russell Kaplan, Justin Johnson, and Li Fei-Fei. Hidden: Hiding data with deep networks. In *European Conference on Computer Vision*, 2018. 3
- Liming Zou, Jing Li, Wenbo Wan, QM Jonathan Wu, and Jiande Sun. Robust coverless image steganography based on neglected coverless image dataset construction. *IEEE Transactions on Multimedia*, 25:5552–5564, 2022. 3